Available online at www.sciencedirect.com
ScienceDirect
Journal of Sound and Vibration 313 (2008) 134–148
JOURNAL OF SOUND AND VIBRATION
www.elsevier.com/locate/jsvi

Three-dimensional vibration analysis of cantilevered skew plates

Ding Zhou[a,*], Weiqing Liu[a,*], Qingli Yang[b]

[a]*College of Civil Engineering, Nanjing University of Technology, Nanjing 210009, People's Republic of China*
[b]*School of Building Engineering, Xinjiang University, 21 Youhao North Road, Urumqi 830008, Xinjiang, People's Republic of China*

Received 23 April 2006; received in revised form 12 October 2007; accepted 11 November 2007
Available online 2 January 2008

Abstract

Three-dimensional (3-D) free vibration of cantilevered thick skew plates is analyzed, based on the exact, linear and small-strain elasticity theory. The skew domain of the plate is mapped onto a cubic domain. A set of triplicate Chebyshev polynomials multiplied by a boundary function is developed as the trial functions of each displacement components. Using the Ritz method, the eigenvalue equation is derived from the strain energy and kinetic energy of the plate. The vibration modes are divided into the antisymmetric and symmetric ones in the thickness direction, therefore, can be studied individually. The convergence study shows that the first eight frequency parameters for each mode categories can be obtained with an accuracy of at least four significant figures. The effect of geometric parameters, such as skew angle, aspect ratio and span-thickness ratio, on frequency parameters is studied. The results are compared with those obtained by using the algebraic polynomials as trial functions and the 3-D finite element solutions, respectively. It is shown that the Chebyshev polynomials can provide better numerical stability than the algebraic polynomials, especially for the plates with large skew angle. The present results can serve as the benchmark data for the accuracy evaluation of other computational techniques.

1. Introduction

There are numerous papers published on static and dynamic analysis of plates with various shapes, most of which were performed by using two-dimensional (2-D) theories such as the classical theory [1] for thin plates, Mindlin theory [2] for moderate thickness plates and high-order theories [3] for thick plates.

In engineering applications, skew plates are frequently used as structural components such as the swept wings, skew bridges and building floors. Their vibration characteristics are obviously important for designers. Since the early 1950s, a lot of studies on the vibration of skew plates have been performed [4–12]. However, most of the studies followed the classical plate theory, applicability of which is subjected to a serious limitation on the plate thickness. In such a case, inaccuracies of results rapidly increase with the increases of the plate thickness. Moreover, corner stress singularities inevitably occur at the obtuse corners and become significant to the vibration analysis with increasing corner angle due to the simplifying representations of the physical problems. For plates with large skew angle, accurate results can be obtained when the conventional trial

*Corresponding authors.
E-mail address: dingzhou57@yahoo.com (D. Zhou).

0022-460X/$ - see front matter © 2007 Elsevier Ltd. All rights reserved.
doi:10.1016/j.jsv.2007.11.016

functions are augmented by sets of corner functions [13,14]. Moreover, some investigates on vibration of skew plates with moderate thickness, based on Mindlin plate theory, have also been carried out [15–17].

Three-dimensional (3-D) analysis of plates has long been a goal for researchers who work in this field. Such an analysis not only provides realistic results but also allows further physical insights, which cannot otherwise be predicted by the 2-D analysis [18,19]. In the recent three decades, some attempts have been made for 3-D vibration analysis of thick plates. Srinivas et al. [20] derived the exact 3-D elasticity solution for free vibration of rectangular plates with all edges simply supported. Hutchinson and Zillmer [21] and Fromme and Leissa [22] developed the respective series solutions to analyze the free vibration of completely free parallelepiped. Furthermore, Leissa and Zhang [23] used the Ritz method to study the 3-D free vibration of cantilevered rectangular parallelepiped and Cheung and Chakrabarti [24] developed the finite layer method to study the vibration of thick rectangular plates with general boundary conditions. In the recent 10 years, some new advances on 3-D vibration analysis of thick plates have been achieved. Malik and Bert [25] and Liew and Teo [26] used the differential quadrature method to analyze the 3-D vibration characteristics of rectangular plates. Zhou et al. [27] used the Chebyshev polynomials and Liew et al. [28] used the orthogonal polynomials as trial functions in the Ritz method to analyze such plates. Moreover, the Ritz method has been extended to investigate the 3-D vibration of plates with other shapes such as triangular plates [29], cantilevered skewed plates [30] and cantilevered trapezoids [31]. Scanning the published literature, one can find that the research on 3-D vibration analysis of skew plates is very limited. Only cantilevered skew plates [32] and fully simply supported skew plates [33] have been investigated.

McGree and Leissa [30] presented the first known solutions of 3-D free vibration for cantilevered skew plates by using the Ritz method. They used a set of triplicate algebraic polynomials as the trial functions, which geometrically satisfies the fixed face conditions. Their results were compared with those obtained by using the 3-D finite elements. It is shown that in some cases, a remarkable disagreement of natural frequencies can be observed between the two methods.

In the present study, the skew domain of the plate is mapped onto a cubic domain and a set of triplicate Chebyshev polynomials multiplied by a boundary function satisfying the geometric boundary conditions of the plates are taken as the trial functions in the Ritz method. Rapid convergence, high accuracy and excellent numerical robustness have been demonstrated. Reliable numerical results have been given for plates with different aspect ratios, span-thickness ratios and skew angles. The results are compared with those obtained by using the algebraic polynomials as trial functions and those obtained by using the 3-D finite elements [30]. It is shown that the present solutions are in agreement with the 3-D finite element solutions for all cases; they however, are different from the algebraic polynomial solutions when the plates are with large skew angles.

2. Theoretical formulation

Consider a skew plate with side lengths a and b, thickness t, and skew angle α with respect to the axis y, as shown in Fig. 1(a). The plate is defined in a right-handed orthogonal coordinate system (x, y, z). The top and bottom surfaces of the plate parallel to the reference median plane x–y. Based on the 3-D, linear and small-strain elasticity theory, the strain energy $\bar{V}$ and the kinetic energy $\bar{T}$ of the plate undergoing a small amplitude vibration are given by the volume integrals

$$\bar{V} = (1/2)\iiint [\lambda(\varepsilon_x + \varepsilon_y + \varepsilon_z)^2 + 2G(\varepsilon_x^2 + \varepsilon_y^2 + \varepsilon_z^2) + G(\gamma_{xy}^2 + \gamma_{yz}^2 + \gamma_{zx}^2)]\,\mathrm{d}x\,\mathrm{d}y\,\mathrm{d}z,$$
$$\bar{T} = (\rho/2)\iiint (\dot{u} + \dot{v} + \dot{w})\,\mathrm{d}x\,\mathrm{d}y\,\mathrm{d}z, \tag{1}$$

where ρ is a constant mass per unit volume; $u = u(x, y, z, \tau)$, $v = v(x, y, z, \tau)$ and $w = w(x, y, z, \tau)$ are displacement components in the x, y and z directions, respectively; $\dot{u}$, $\dot{v}$ and $\dot{w}$ are their corresponding velocity components, which are, respectively, the derivatives of each displacement components with respect to the time variable τ. λ and G are the Lamè constants for a homogeneous and isotropic material, which are expressed in terms of Young's modulus E and the Poisson's ratio v by

$$\lambda = vE/[(1 + v)(1 - 2v)], \quad G = E/[2(1 + v)]. \tag{2}$$

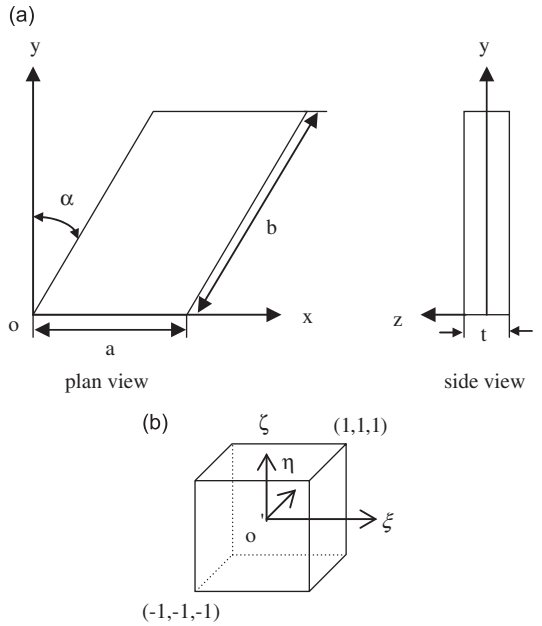

Fig. 1. Geometry, dimensions, coordinates and domain transformation: (a) skew plate and (b) cubic domain.

In Eq. (1), the linear strain–placement relations are given by

$$\varepsilon_x = \partial u/\partial x, \quad \varepsilon_y = \partial v/\partial y, \quad \varepsilon_z = \partial w/\partial z,$$

$$\gamma_{xy} = \partial v/\partial x + \partial u/\partial y, \quad \gamma_{yz} = \partial w/\partial y + \partial v/\partial z, \quad \gamma_{zx} = \partial u/\partial z + \partial w/\partial x. \tag{3}$$

The skew domain of the plate can be mapped onto a basic cubic domain, as shown in Fig. 1(b), using the following coordinate transformation:

$$x = a(\xi + \eta \sin\alpha/\beta + 1 + \sin\alpha/\beta)/2, \quad y = b(\eta + 1)\cos\alpha/2, \quad z = t\zeta/2, \tag{4}$$

where $\beta = a/b$ is the side-length ratio of the plate. Applying the chain rule of differentiation, the relation of the first derivative in the two coordinate systems x–y–z and ξ–η–ζ can be expressed as

$$\begin{Bmatrix} \dfrac{\partial()}{\partial x} \\ \dfrac{\partial()}{\partial y} \end{Bmatrix} = \bar{J}^{-1} \begin{Bmatrix} \dfrac{\partial()}{\partial \xi} \\ \dfrac{\partial()}{\partial \eta} \end{Bmatrix}, \quad \frac{\partial()}{\partial z} = \frac{t}{2}\frac{\partial()}{\partial \zeta}, \tag{5}$$

where

$$\bar{J} = \begin{bmatrix} \dfrac{\partial x}{\partial \xi} & \dfrac{\partial y}{\partial \xi} \\ \dfrac{\partial x}{\partial \eta} & \dfrac{\partial y}{\partial \eta} \end{bmatrix} = \frac{a}{2}\begin{bmatrix} 1 & 0 \\ \sin\alpha/\beta & \cos\alpha/\beta \end{bmatrix}, \tag{6}$$

in which, $\bar{J}$ denotes the Jacobian matrix of the geometrical mapping. Eqs. (5) and (6) will be used to transform the integration in the x–y–z domain into those in the ξ–η–ζ domain.

For free vibrations, the displacement components of a 3-D elastic body may be expressed as

$$u = U(\xi,\eta,\zeta)e^{i\omega\tau}, \quad v = V(\xi,\eta,\zeta)e^{i\omega\tau}, \quad w = W(\xi,\eta,\zeta)e^{i\omega\tau}, \tag{7}$$

where ω is the circular eigenfrequency of vibration and $i = \sqrt{-1}$.

Substituting Eqs. (3)–(7) into Eq. (1), the energy functional $\bar{L}$ of the plate can be expressed as

$$\bar{L} = \bar{V}_{\max} - \bar{T}_{\max} = \frac{tb}{4a}\cos\alpha \int_{-1}^{1}\int_{-1}^{1}\int_{-1}^{1}[\lambda\bar{V}_1 + G(\bar{V}_2 + \bar{V}_3)]\,\mathrm{d}\xi\,\mathrm{d}\eta\,\mathrm{d}\zeta - \frac{abt}{16}\cos\alpha\rho\omega^2 \int_{-1}^{1}\int_{-1}^{1}\int_{-1}^{1}(U^2 + V^2 + W^2)\,\mathrm{d}\xi\,\mathrm{d}\eta\,\mathrm{d}\zeta, \tag{8}$$

where

$$\begin{aligned}
\bar{V}_1 &= (\partial U/\partial\xi - \tan\alpha\partial V/\partial\xi + \sec\alpha\beta\partial V/\partial\eta + \gamma\,\partial W/\partial\zeta)^2,\\
\bar{V}_2 &= 2(\partial U/\partial\xi)^2 + 2(\tan\alpha\,\partial V/\partial\xi - \sec\alpha\beta\,\partial V/\partial\eta)^2 + 2(\gamma\,\partial W/\partial\zeta)^2,\\
\bar{V}_3 &= (\tan\alpha\,\partial U/\partial\xi - \sec\alpha\beta\,\partial U/\partial\eta - \partial V/\partial\xi)^2\\
&\quad + (\gamma\,\partial V/\partial\zeta - \tan\alpha\,\partial W/\partial\xi + \sec\alpha\beta\,\partial W/\partial\eta)^2 + (\partial W/\partial\xi + \gamma\,\partial U/\partial\zeta)^2,
\end{aligned} \tag{9}$$

in which, $\gamma = a/t$ is referred as to the span-thickness ratio of the plate.

In the present analysis, the displacement functions U, V and W of the plates are approximately expressed in terms of a finite triplicate series:

$$\begin{aligned}
U(\xi,\eta,\zeta) &= (1+\xi)\sum_{i=1}^{I}\sum_{j=1}^{J}\sum_{k=1}^{K} A_{ijk}F_i(\xi)F_j(\eta)F_k(\zeta),\\
V(\xi,\eta,\zeta) &= (1+\xi)\sum_{l=1}^{L}\sum_{m=1}^{M}\sum_{n=1}^{N} B_{lmn}F_l(\xi)F_m(\eta)F_n(\zeta),\\
W(\xi,\eta,\zeta) &= (1+\xi)\sum_{p=1}^{P}\sum_{q=1}^{Q}\sum_{r=1}^{R} C_{pqr}F_p(\xi)F_q(\eta)F_r(\zeta),
\end{aligned} \tag{10}$$

where A_{ijk}, B_{lmn} and C_{pqr} are undetermined coefficients, $1+\xi$ refers to as the boundary function which ensures the exact satisfaction of the geometric boundary conditions of the cantilevered skew plates. The series functions have an identical form: $F_s(\chi)$ ($s = i,j,k,l,m,n,p,q,r$ and $\chi = \xi,\eta,\zeta$) which are a set of Chebyshev polynomials defined in the interval $[-1, 1]$, expressed by

$$F_s(\chi) = \cos[(s-1)\arccos(\chi)],\ s = 1,2,3,\ldots. \tag{11}$$

The first five Chebyshev polynomials are given in Fig. 2. It should be noted that selecting Chebyshev polynomial series as the trial functions of displacement components has three distinct advantages [33]. The first advantage is that $F_s(\chi)$ ($s = 1, 2, 3, \ldots$) is a set of complete and orthogonal series in the interval $[-1, 1]$. This ensures the triplicate series $F_i(\xi)F_j(\eta)F_k(\zeta)$ ($i, j, k = 1, 2, 3, \ldots$) to form a complete and orthogonal set in the cubic domain. It is obvious that the boundary function destroys the orthogonality of the admissible functions. The main properties of Chebyshev polynomials, such as the numerical robustness in computations, are still preserved in the admissible functions because the boundary function is invariable in sign. The second advantage is that Chebyshev polynomials have the more rapid convergence and better numerical robustness than other polynomial series such as simply polynomials. The third advantage is that $F_s(\chi)$ ($s = 1, 2, 3, \ldots$) can be expressed into a unified form of cosine functions, which could reduce the coding effort.

Substituting Eqs. (9) and (10) into Eq. (8), and minimizing $\bar{L}$ with respect to the undetermined coefficients A_{ijk}, B_{lmn} and C_{pqr}, a set of eigenfrequency equations is derived, which can be written in matrix form as

$$\left(\begin{bmatrix} [K_{uu}] & [K_{uv}] & [K_{uw}] \\ [K_{uv}]^{\mathrm{T}} & [K_{vv}] & [K_{vw}] \\ [K_{uw}]^{\mathrm{T}} & [K_{vw}]^{\mathrm{T}} & [K_{ww}] \end{bmatrix} - \Lambda^2 \begin{bmatrix} M_{uu} & 0 & 0 \\ 0 & M_{vv} & 0 \\ 0 & 0 & M_{ww} \end{bmatrix}\right)\begin{Bmatrix} \{A\} \\ \{B\} \\ \{C\} \end{Bmatrix} = \begin{Bmatrix} \{0\} \\ \{0\} \\ \{0\} \end{Bmatrix}, \tag{12}$$

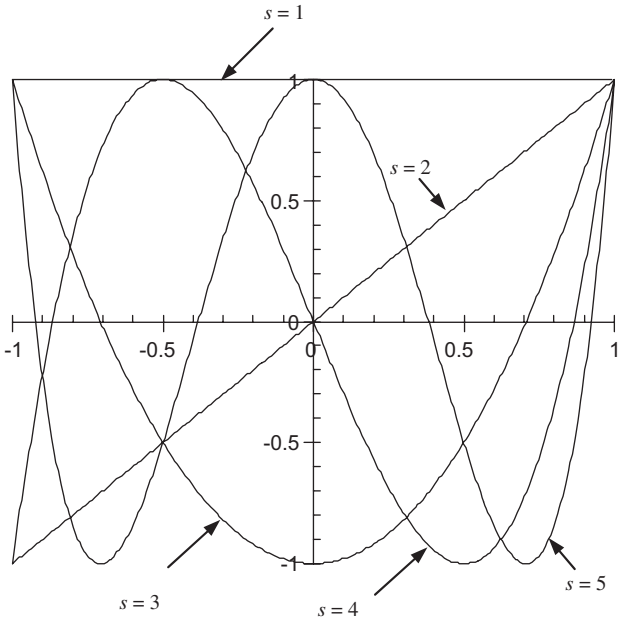

Fig. 2. The first five terms of the Chebyshev polynomials $F_s(\chi)$ ($s = 1, 2, 3, 4, 5$).

Table 1
The convergence of the first eight frequency parameters for the antisymmetric modes in the thickness direction, $\alpha = 30^\circ$ and $\beta = 1$

$I \times J \times K$	Ω_1	Ω_2	Ω_3	Ω_4	Ω_5	Ω_6	Ω_7	Ω_8
$\gamma = 100/3$								
$10 \times 10 \times 2$	3.930	9.336	25.12	25.75	40.77	50.00	71.36	72.28
$10 \times 10 \times 3$	3.930	9.336	25.12	25.75	40.77	50.00	71.36	72.28
$13 \times 13 \times 1$	4.243	9.633	26.11	27.51	42.87	53.72	75.44	76.06
$13 \times 13 \times 2$	3.923	9.319	25.06	25.71	40.69	49.91	71.19	72.17
$13 \times 13 \times 3$	3.923	9.319	25.06	25.71	40.69	49.91	71.19	72.17
$16 \times 16 \times 2$	3.919	9.311	25.04	25.70	40.66	49.88	71.13	72.12
$16 \times 16 \times 3$	3.919	9.311	25.04	25.70	40.66	49.88	71.13	72.12
$19 \times 19 \times 1$	4.241	9.626	26.09	27.50	42.85	53.70	75.38	75.99
$19 \times 19 \times 2$	3.918	9.308	25.03	25.70	40.66	49.87	71.11	72.11
$22 \times 22 \times 1$	4.241	9.626	26.09	27.49	42.85	53.69	75.38	75.98
$22 \times 22 \times 2$	3.917	9.307	25.03	25.69	40.65	49.87	71.09	72.10
$22 \times 22 \times 3$	3.917	9.307	25.03	25.69	40.65	49.87	71.09	72.10
$25 \times 25 \times 2$	3.917	9.307	25.03	25.69	40.65	49.87	71.09	72.10
$\gamma = 10/3$								
$7 \times 7 \times 4$	3.578	7.254	16.26	18.59	25.27	30.62	36.46	39.41
$7 \times 7 \times 5$	3.578	7.254	16.26	18.59	25.27	30.62	36.46	39.41
$9 \times 9 \times 3$	3.571	7.248	16.24	18.58	25.26	30.60	36.41	39.32
$9 \times 9 \times 4$	3.571	7.247	16.24	18.58	25.26	30.60	36.40	39.32
$9 \times 9 \times 5$	3.571	7.247	16.24	18.58	25.26	30.60	36.40	39.32
$11 \times 11 \times 4$	3.568	7.245	16.23	18.57	25.25	30.59	36.39	39.31
$11 \times 11 \times 5$	3.568	7.245	16.23	18.57	25.25	30.59	36.39	39.31
$13 \times 13 \times 3$	3.567	7.245	16.23	18.58	25.26	30.59	36.39	39.31
$13 \times 13 \times 4$	3.566	7.244	16.23	18.57	25.25	30.59	36.38	39.30
$15 \times 15 \times 3$	3.566	7.245	16.23	18.58	25.26	30.59	36.39	39.31
$15 \times 15 \times 4$	3.565	7.243	16.23	18.57	25.25	30.59	36.38	39.30
$15 \times 15 \times 5$	3.565	7.243	16.23	18.57	25.25	30.59	36.38	39.30
$17 \times 17 \times 4$	3.564	7.243	16.23	18.57	25.25	30.59	36.38	39.30
$19 \times 19 \times 4$	3.564	7.243	16.23	18.57	25.25	30.59	36.38	39.30

in which $\Lambda = \omega a\sqrt{\rho/E}$, $[K_{ij}]$ and $[M_{ii}](i,j = u,v,w)$ are the sub-stiffness matrices and the sub-mass matrices, respectively. $\{A\}$, $\{B\}$ and $\{C\}$ are the column vectors of the unknown coefficients which are expressed as

$$\{A\} = \begin{Bmatrix} A_{111} \\ A_{112} \\ \vdots \\ A_{11K} \\ A_{121} \\ \vdots \\ A_{12K} \\ \vdots \\ A_{1JK} \\ \vdots \\ A_{IJK} \end{Bmatrix}, \quad \{B\} = \begin{Bmatrix} B_{111} \\ B_{112} \\ \vdots \\ B_{11N} \\ B_{121} \\ \vdots \\ B_{12N} \\ \vdots \\ B_{1MN} \\ \vdots \\ A_{LMN} \end{Bmatrix}, \quad \{C\} = \begin{Bmatrix} C_{111} \\ C_{112} \\ \vdots \\ C_{11R} \\ C_{121} \\ \vdots \\ C_{12R} \\ \vdots \\ C_{1QR} \\ \vdots \\ C_{PQR} \end{Bmatrix}. \tag{13}$$

Table 2
The convergence of the first eight frequency parameters for the symmetric modes in the thickness direction, $\alpha = 30^\circ$ and $\beta = 1$

$I \times J \times K$	Ω_1	Ω_2	Ω_3	Ω_4	Ω_5	Ω_6	Ω_7	Ω_8
$\gamma = 100/3$								
$10 \times 10 \times 2$	73.67	163.5	210.4	303.6	338.6	399.7	446.6	500.5
$10 \times 10 \times 3$	73.67	163.5	210.4	303.6	338.6	399.7	446.6	500.5
$13 \times 13 \times 2$	73.54	163.5	210.2	303.6	338.5	399.7	446.4	500.5
$13 \times 13 \times 3$	73.54	163.5	210.2	303.6	338.5	399.7	446.4	500.5
$16 \times 16 \times 1$	73.49	163.5	210.1	303.6	338.5	399.7	446.4	500.5
$16 \times 16 \times 2$	73.48	163.5	210.1	303.5	338.5	399.7	446.3	500.5
$16 \times 16 \times 3$	73.48	163.5	210.1	303.5	338.5	399.7	446.3	500.5
$19 \times 19 \times 1$	73.46	163.5	210.1	303.6	338.5	399.7	446.3	500.5
$19 \times 19 \times 2$	73.45	163.5	210.0	303.5	338.5	399.7	446.3	500.5
$22 \times 22 \times 1$	73.45	163.5	210.0	303.6	338.5	399.7	446.3	500.5
$22 \times 22 \times 2$	73.44	163.5	210.0	303.5	338.5	399.7	446.2	500.5
$22 \times 22 \times 3$	73.44	163.5	210.0	303.5	338.5	399.7	446.2	500.5
$25 \times 25 \times 2$	73.44	163.5	210.0	303.5	338.5	399.7	446.2	500.5
$\gamma = 10/3$								
$7 \times 7 \times 4$	7.436	16.37	21.14	30.34	33.86	39.91	44.61	49.96
$7 \times 7 \times 5$	7.436	16.37	21.14	30.34	33.86	39.91	44.61	49.96
$9 \times 9 \times 3$	7.410	16.37	21.11	30.34	33.84	39.89	44.56	49.91
$9 \times 9 \times 4$	7.409	16.37	21.10	30.34	33.84	39.89	44.55	49.91
$9 \times 9 \times 5$	7.409	16.37	21.10	30.34	33.84	39.89	44.55	49.91
$11 \times 11 \times 4$	7.397	16.37	21.09	30.34	33.83	39.89	44.54	49.91
$11 \times 11 \times 5$	7.397	16.37	21.09	30.34	33.83	39.89	44.54	49.91
$13 \times 13 \times 3$	7.392	16.37	21.08	30.34	33.83	39.89	44.53	49.91
$13 \times 13 \times 4$	7.391	16.37	21.08	30.34	33.83	39.89	44.53	49.90
$15 \times 15 \times 3$	7.388	16.37	21.07	30.34	33.83	39.89	44.52	49.90
$15 \times 15 \times 4$	7.388	16.37	21.07	30.34	33.83	39.89	44.52	49.90
$15 \times 15 \times 5$	7.388	16.37	21.07	30.34	33.83	39.89	44.52	49.90
$17 \times 17 \times 4$	7.386	16.37	21.07	30.34	33.83	39.89	44.52	49.90
$19 \times 19 \times 4$	7.386	16.37	21.07	30.34	33.83	39.89	44.52	49.90

Every elements in sub-matrices $[K_{ij}]$ and $[M_{ii}]$ $(i,j=u,v,w)$ are given by

$$[K_{uu}]=[(1-\nu)/(1-2\nu)+\tan^2\alpha/2]E^{11}_{uiu\bar{i}}G^{00}_{uju\bar{j}}H^{00}_{uku\bar{k}}+\beta^2\sec^2\alpha E^{00}_{uiu\bar{i}}G^{11}_{uju\bar{j}}H^{00}_{uku\bar{k}}/2 -\beta\tan\alpha\sec\alpha(E^{10}_{uiu\bar{i}}G^{01}_{uju\bar{j}}+E^{01}_{uiu\bar{i}}G^{10}_{uju\bar{j}})H^{00}_{uku\bar{k}}/2+\gamma^2E^{00}_{uiu\bar{i}}G^{00}_{uju\bar{j}}H^{11}_{uku\bar{k}}/2,$$

$$[K_{vv}]=\beta^2\sec^2\alpha(1-\nu)E^{00}_{vlv\bar{l}}G^{11}_{vmv\bar{m}}H^{00}_{vnv\bar{n}}/(1-2\nu)+\gamma^2E^{00}_{vlv\bar{l}}G^{00}_{vmv\bar{m}}H^{11}_{vnv\bar{n}}/2 +[\tan^2\alpha(1-\nu)/(1-2\nu)+0.5]E^{11}_{vlv\bar{l}}G^{00}_{vmv\bar{m}}H^{00}_{vnv\bar{n}} -\beta\tan\alpha\sec\alpha(1-\nu)(E^{10}_{vlv\bar{l}}G^{01}_{vmv\bar{m}}+E^{01}_{vlv\bar{l}}G^{10}_{vmv\bar{m}})H^{00}_{vnv\bar{n}}/(1-2\nu),$$

$$[K_{ww}]=\gamma^2(1-\nu)E^{00}_{wpw\bar{p}}G^{00}_{wqw\bar{q}}H^{11}_{wrw\bar{r}}/(1-2\nu)+\beta^2\sec^2\alpha E^{00}_{wpw\bar{p}}G^{11}_{wqw\bar{q}}H^{00}_{wrw\bar{r}}/2 \times(1+\tan^2\alpha)E^{11}_{wpw\bar{p}}G^{00}_{wqw\bar{q}}H^{00}_{wrw\bar{r}}/2-\beta\tan\alpha\sec\alpha(E^{10}_{wpw\bar{p}}G^{01}_{wqw\bar{q}}+E^{01}_{wpw\bar{p}}G^{10}_{wqw\bar{q}})H^{00}_{wrw\bar{r}}/2,$$

$$[K_{uv}]=\beta\sec\alpha[\nu E^{10}_{uiv\bar{l}}G^{01}_{ujv\bar{m}}/(1-2\nu)+E^{01}_{uiv\bar{l}}G^{10}_{ujv\bar{m}}/2]H^{00}_{ukv\bar{n}}-\tan\alpha[\nu/(1-2\nu)+0.5]E^{11}_{uiv\bar{l}}G^{00}_{ujv\bar{m}}H^{00}_{ukv\bar{n}},$$

$$[K_{uw}]=\gamma[\nu E^{10}_{uiw\bar{p}}H^{01}_{ukw\bar{r}}/(1-2\nu)+E^{01}_{uiw\bar{p}}H^{10}_{ukw\bar{r}}/2]G^{00}_{ujw\bar{q}},$$

$$[K_{vw}]=\beta\gamma\sec\alpha[\nu G^{10}_{vmw\bar{q}}H^{01}_{vnw\bar{r}}/(1-2\nu)+G^{01}_{vmw\bar{q}}H^{10}_{vnw\bar{r}}/2]E^{00}_{vlw\bar{p}} -\gamma\tan\alpha[\nu E^{10}_{vlw\bar{p}}H^{01}_{vnw\bar{r}}/(1-2\nu)+E^{01}_{vlw\bar{p}}H^{10}_{vnw\bar{r}}/2]G^{00}_{vmw\bar{q}},$$

Table 3
The first eight frequency parameters for skewed, cantilevered thick plates with aspect ratio $\beta=0.5$ and span-thickness ratio $\gamma=1$

Mode	Method	$\alpha=0^\circ$	$\alpha=15^\circ$	$\alpha=30^\circ$	$\alpha=45^\circ$
Ω_1	Present	2.2201	2.2585	2.3617	2.5155
	Ref. [30]	2.2304	2.2987	2.5790	3.1205
	3-D FE	2.2375	2.2757	2.3791	2.5398
Ω_2	Present	2.7073	2.7453*	2.7636*	2.6103*
	Ref. [30]	2.7039	2.8662	3.3293	4.1110
	3-D FE	2.6884	2.7535	2.7861	2.6920
Ω_3	Present	2.7239*	2.7899	3.0815	3.5952
	Ref. [30]	2.7577	2.8973	3.4345	4.8256
	3-D FE	2.7289	2.7675	3.0452	3.4531
Ω_4	Present	4.4629	4.5038	4.5654	4.4254
	Ref. [30]	4.7438	4.8997	5.3477	6.6697
	3-D FE	4.2550	4.2921	4.3260	4.3008
Ω_5	Present	5.0539*	4.8523*	4.6032*	4.5860*
	Ref. [30]	5.0722	5.0376	5.4416	6.8077
	3-D FE	5.0096	4.8003	4.5566	4.5895
Ω_6	Present	5.5551*	5.5318	5.3506	5.5869
	Ref. [30]	5.5855	5.8947	6.6160	8.1640
	3-D FE	5.5375	5.1834	5.0861	5.3187
Ω_7	Present	5.5813*	5.6596*	6.0684*	6.4360*
	Ref. [30]	5.5932	5.9298	7.1205	9.7608
	3-D FE	5.5698	5.8741	5.9334	5.4364
Ω_8	Present	5.7101	5.8757*	6.3335*	6.8575*
	Ref. [30]	5.8219	6.1000	7.3500	10.0930
	3-D FE	5.7046	5.7498	6.1511	6.5378

Note: Data with superscript (*) mean the symmetric modes in the thickness direction.

$$[M_{uu}] = (1+v)E^{00}_{uiu\bar{i}}G^{00}_{uju\bar{j}}H^{00}_{uku\bar{k}}/4,$$
$$[M_{vv}] = (1+v)E^{00}_{vlv\bar{l}}G^{00}_{vmv\bar{m}}H^{00}_{vnv\bar{n}}/4,$$
$$[M_{ww}] = (1+v)E^{00}_{vpv\bar{p}}G^{00}_{vqv\bar{q}}H^{00}_{wrw\bar{r}}/4, \tag{14}$$

in which

$$E^{\theta\sigma}_{\tau s\varsigma\bar{s}} = \int_{-1}^{1}\{\mathrm{d}^{\theta}[(1+\xi)F_s(\xi)]/\mathrm{d}\xi^{\theta}\}\{\mathrm{d}^{\sigma}[(1+\xi)F_{\bar{s}}(\xi)]/\mathrm{d}\xi^{\sigma}\}\,\mathrm{d}\xi,$$
$$G^{\theta\sigma}_{\tau s\varsigma\bar{s}} = \int_{-1}^{1}[\mathrm{d}^{\theta}F_s(\eta)/\mathrm{d}\eta^{\theta}]\{\mathrm{d}^{\sigma}F_{\bar{s}}(\eta)/\mathrm{d}\eta^{\sigma}]\,\mathrm{d}\eta,$$
$$H^{\theta\sigma}_{\tau s\varsigma\bar{s}} = \int_{-1}^{1}[\mathrm{d}^{\theta}F_s(\zeta)/\mathrm{d}\zeta^{\theta}][\mathrm{d}^{\sigma}F_{\bar{s}}(\zeta)/\mathrm{d}\zeta^{\sigma}]\,\mathrm{d}\zeta,$$
$$\theta,\sigma = 0,1, \quad \tau,\varsigma = u,v,w, \quad s = i,j,k,l,m,n,p,q,r,$$
$$\bar{s} = \bar{i},\bar{j},\bar{k},\bar{l},\bar{m},\bar{n},\bar{p},\bar{q},\bar{r}. \tag{15}$$

A non-trivial solution can be obtained by setting the determinant of the coefficient matrix in Eq. (12) equal to zero. Roots of the determinant are the square of the eigenvalue Λ (dimensionless eigenfrequency). Eigenfunctions, i.e. mode shapes, corresponding to every eigenvalues could be determined by back-substitution of the eigenvalues, one by one, in the usual manner.

Table 4
The first eight frequency parameters for skewed, cantilevered thick plates with aspect ratio $\beta = 0.5$ and span-thickness ratio $\gamma = 2.5$

Mode	Method	$\alpha = 0^\circ$	$\alpha = 15^\circ$	$\alpha = 30^\circ$	$\alpha = 45^\circ$
Ω_1	Present	3.1201	3.2169	3.4755	3.8085
	Ref. [30]	3.1227	3.2166	3.5510	4.1425
	3-D FE	3.1238	3.2217	3.4885	3.8582
Ω_2	Present	4.2737	4.4007	4.9113	6.2795
	Ref. [30]	4.2261	4.3542	5.0753	7.1414
	3-D FE	4.2821	4.4073	4.9183	6.2958
Ω_3	Present	6.7831*	6.8335*	6.8679*	6.4618*
	Ref. [30]	6.8552	7.2038	8.2730	10.2007
	3-D FE	6.7974	6.8581	6.9365	6.6924
Ω_4	Present	7.4367	7.5818	8.0905	9.2646
	Ref. [30]	8.0642	8.3654	9.3562	11.4351
	3-D FE	7.3213	7.4760	8.0192	9.2653
Ω_5	Present	12.6109*	12.1137*	11.4863*	11.4371*
	Ref. [30]	12.6494	12.5656	13.3447	16.6312
	3-D FE	12.5705	12.0459	11.4246	11.5383
Ω_6	Present	12.6290	12.7055	13.0946	13.6847
	Ref. [30]	12.9342	12.9723	14.7501	18.9970
	3-D FE	12.9816	12.3409	12.7782	13.3430
Ω_7	Present	13.0500	13.3018	13.6728	14.2504
	Ref. [30]	13.5239	14.3488	17.1083	22.5717
	3-D FE	13.3094	13.1870	13.5041	14.2523
Ω_8	Present	13.9514*	14.1777	15.2067*	16.1010*
	Ref. [30]	13.9620	14.7390	17.7850	24.5030
	3-D FE	14.4315	14.3078	15.1933	16.7757

Note: Data with superscript (*) mean the symmetric modes in the thickness direction.

It can be seen from Fig. 2 that the Chebyshev polynomials is symmetric for $s = 1, 3, 5, \ldots$ and antisymmetric for $s = 2, 4, 6, \ldots$. Therefore, the symmetric and antisymmetric modes of skew plates in the thickness direction can be individually studied, which reduces the computational cost.

3. Convergence study

It is well known that the Ritz method provides the upper bound of eigenfrequencies. The efficiency of the method depends on the type of trial functions adopted in the analysis. Solution of any accuracy could be obtained theoretically by using sufficient number of terms of trial functions. However, a limit to the number of terms of trial functions always exists because of the limited speed, the capacity and the numerical accuracy of computers. In the 3-D analysis of elastic bodies, numerical instability would occur when a great number of terms of trial functions are used, especially in the case of the triplicate series having to be used. In the dynamic analysis, a typical numerical instability is the ill-conditioned eigenvalues, the earlier or later occurrence of which is concerned with the trial functions used in the calculation. Therefore, the validity of a Ritz solution often is enslaved to the convergence rate, the numerical stability and the accuracy of the method.

A convergence study is performed for eigenfrequencies of cantilevered skew plates with the aspect ratio $\beta = 1$ (rhombic) and skew angle $\alpha = 30^\circ$. For simplicity, the same number of Chebyshev polynomials in each displacement components U, V and W are used, though more efficient computation can be achieved, otherwise. This implies that $I = L = P$; $J = M = Q$ and $K = N = R$. Two different span-thickness ratios, $\gamma = 100/3$ (corresponding to a thin plate) and $\gamma = 10/3$ (corresponding to a thick plate), are considered. The computations are carried out in Pentium IV microcomputer with double precision and the integrals in Eq. (15)

Table 5
The first eight frequency parameters for skewed, cantilevered thick plates with aspect ratio $\beta = 1$ and span-thickness ratio $\gamma = 2$

Mode	Method	$\alpha = 0^\circ$	$\alpha = 15^\circ$	$\alpha = 30^\circ$	$\alpha = 45^\circ$
Ω_1	Present	2.9338	2.9936	3.1656	3.4266
	Ref. [30]	2.9463	3.0096	3.3164	3.8412
	3-D FE	2.9397	3.0017	3.1809	3.4554
Ω_2	Present	4.3881*	4.4123*	4.4526*	4.3678*
	Ref. [30]	4.4178	4.6232	4.6768	6.5555
	3-D FE	4.3957	4.4244	4.4802	4.4421
Ω_3	Present	5.1926	5.3058	5.7115	6.6142
	Ref. [30]	5.1815	5.3635	6.1756	7.6914
	3-D FE	5.1470	5.2527	5.6351	6.4876
Ω_4	Present	10.5174*	10.2762*	9.8318*	9.3982*
	Ref. [30]	10.5391	9.9399	11.3566	13.3667
	3-D FE	10.5200	10.2640	9.8067	9.4300
Ω_5	Present	10.9370	11.0326	11.2157	11.1608
	Ref. [30]	10.9792	10.6450	13.5265	18.6951
	3-D FE	10.7864	10.8493	10.9455	10.8145
Ω_6	Present	11.7083*	12.0385*	12.6656*	12.9708*
	Ref. [30]	11.7535	11.3436	13.5265	18.6951
	3-D FE	11.6626	12.0043	12.6506	13.0694
Ω_7	Present	14.5991	14.1467	14.0736	14.4686
	Ref. [30]	14.4674	12.5292	14.3425	18.9918
	3-D FE	14.3273	13.7176	13.6732	14.0382
Ω_8	Present	15.0238	15.9727	17.2395	17.4823
	Ref. [30]	16.1660	14.4180	15.9530	25.3940
	3-D FE	14.4794	15.3277	16.5283	16.7953

Note: Data with superscript (*) mean the symmetric modes in the thickness direction.

are numerically evaluated by the piecewise Gaussian quadrature of 24 points. Considering the conventional usage in 2-D vibration analysis of plates, a standard dimensionless frequency parameter $\Omega = \omega a^2\sqrt{\rho t/D}$ is used where $D = Et^3/[12(1-\nu^2)]$ is the flexural rigidity of the plate. In all the following computations, the Poisson's ratio is fixed at $\nu = 0.3$. Tables 1 and 2 give, respectively, the convergence of the first eight frequency parameters of antisymmetric and symmetric modes in the thickness direction with respect to the term numbers of the Chebyshev polynomials. It is shown that $22 \times 22 \times 2$ terms for the thin plate ($\gamma = 100/3$) and $17 \times 17 \times 4$ terms for the thick plate ($\gamma = 10/3$) can give the results at least accurate to four significant figures. It can be seen that with the increase of the plate thickness, the reducing number of terms of Chebyshev polynomials in the median surface direction, which corresponds to the more number of terms of Chebyshev polynomials in the thickness direction, should be used to obtain the satisfactory accuracy.

4. Numerical results

Based on the convergence study in the last section, the first eight frequency parameters of cantilevered skew plates are reported in Tables 3–8, respectively. Six cases are considered: (a) plates with aspect ratio $\beta = 0.5$ and span-thickness ratio $\gamma = 1$; (b) plates with aspect ratio $\beta = 0.5$ and span-thickness ratio $\gamma = 2.5$; (c) plates with aspect ratio $\beta = 1$ and span-thickness ratio $\gamma = 2$; (d) plates with aspect ratio $\beta = 1$ and span-thickness ratio $\gamma = 5$; (e) plates with aspect ratio $\beta = 2$ and span-thickness ratio $\gamma = 4$; (f) plates with aspect ratio $\beta = 2$ and span-thickness ratio $\gamma = 10$. The results are compared with those reported in Ref. [30] where both the 3-D algebraic polynomial solution and the 3-D finite element (MSC/NASTRAN CHEXA element, $14 \times 14 \times 3$ mesh) were given.

Table 6
The first eight frequency parameters for skewed, cantilevered thick plates with aspect ratio $\beta = 1$ and span-thickness ratio $\gamma = 5$

Mode	Method	$\alpha = 0^\circ$	$\alpha = 15^\circ$	$\alpha = 30^\circ$	$\alpha = 45^\circ$
Ω_1	Present	3.3554	3.4519	3.7406	4.1970
	Ref. [30]	3.3687	3.3989	3.7583	4.2809
	3-D FE	3.3624	3.4650	3.7740	4.2679
Ω_2	Present	7.3754	7.5250	8.0955	9.5775
	Ref. [30]	7.3397	7.5411	8.2944	10.4206
	3-D FE	7.3941	7.5446	8.1276	9.6755
Ω_3	Present	10.9203*	10.9776*	11.0687*	10.8402*
	Ref. [30]	10.9847	11.5005	11.8183	11.2917
	3-D FE	10.9436	11.0146	11.1511	11.0507
Ω_4	Present	17.7010	18.2223	19.7032	20.9666
	Ref. [30]	17.6949	18.0708	20.3724	23.5901
	3-D FE	17.6728	18.2053	19.7461	21.1558
Ω_5	Present	22.5574	21.7277	21.4716	23.4716*
	Ref. [30]	23.6885	21.9487	22.5723	27.4819
	3-D FE	22.1487	21.4572	21.2757	23.5722
Ω_6	Present	24.0371	25.6249*	24.5449*	23.7282
	Ref. [30]	24.9997	25.5651	28.3452	33.4636
	3-D FE	23.9502	25.6132	24.4965	23.6375
Ω_7	Present	26.1985*	26.1574	30.8163	32.3017*
	Ref. [30]	26.2343	26.3655	31.3633	43.8769
	3-D FE	26.2278	25.9579	30.6623	32.6347
Ω_8	Present	29.2842*	30.0741*	31.5920*	36.6317
	Ref. [30]	29.3881	30.6082	33.8068	47.2720
	3-D FE	29.1873	30.0154	31.6052	36.7692

Note: Data with superscript (*) mean the symmetric modes in the thickness direction.

Table 7
The first eight frequency parameters for skewed, cantilevered thick plates with aspect ratio $\beta = 2$ and span-thickness ratio $\gamma = 4$

Mode	Method	$\alpha = 0^\circ$	$\alpha = 15^\circ$	$\alpha = 30^\circ$	$\alpha = 45^\circ$
Ω_1	Present	3.2609	3.3113	3.4570	3.6807
	Ref. [30]	3.2545	3.2823	3.2943	3.3134
	3-D FE	3.2667	3.3220	3.4865	3.7563
Ω_2	Present	5.7835*	5.7217*	5.5015*	5.0137*
	Ref. [30]	5.7869	5.8978	5.9928	6.6404
	3-D FE	5.7970	5.7466	5.5692	5.2041
Ω_3	Present	10.0470	10.2186	10.8031	11.9752
	Ref. [30]	9.9090	9.8656	10.4693	11.0825
	3-D FE	9.9270	10.0899	10.6543	11.8026
Ω_4	Present	16.4511	16.6957	17.3625	18.2238
	Ref. [30]	16.3311	16.3082	17.4151	19.7762
	3-D FE	16.4537	16.7024	17.3983	18.3928
Ω_5	Present	20.9414*	20.2754*	19.4367*	18.5919*
	Ref. [30]	20.9459	20.9449	21.8063	25.7577
	3-D FE	20.9648	20.2626	19.4645	18.9263
Ω_6	Present	21.9394*	22.7351*	23.7968*	24.3095*
	Ref. [30]	21.9266	23.5630	25.7634	32.3171
	3-D FE	21.8993	22.7818	24.0112	24.8581
Ω_7	Present	30.0260	30.0086	30.4100	32.0305
	Ref. [30]	29.5524	28.8472	30.5295	34.1152
	3-D FE	29.5814	29.6120	30.1386	31.9981
Ω_8	Present	37.6152	38.4286	40.3084	39.7404*
	Ref. [30]	37.2420	30.8320	34.8060	45.4330
	3-D FE	37.4149	38.1270	39.7678	41.1186

Note: Data with superscript (*) mean the symmetric modes in the thickness direction.

From Tables 3 to 8, it is shown that the first five differences between the 3-D finite element solutions and the present solutions are orderly −15.5% (Ω_4 when $\beta = 0.5$, $\gamma = 1$ and $\alpha = 45^\circ$); 9.0% (Ω_1 when $\beta = 2$, $\gamma = 10$ and $\alpha = 45^\circ$); 6.5% (Ω_4 when $\beta = 2$, $\gamma = 10$ and $\alpha = 45^\circ$); −6.3% (Ω_6 when $\beta = 0.5$, $\gamma = 1$ and $\alpha = 15^\circ$) and −5.2% (Ω_4 when $\beta = 0.5$, $\gamma = 1$ and $\alpha = 30^\circ$). However, the first five differences between the algebraic polynomial solutions and the present solutions are orderly 67.5% (Ω_5 when $\beta = 1$, $\gamma = 2$ and $\alpha = 45^\circ$); 58.4% (Ω_8 when $\beta = 0.5$, $\gamma = 2.5$ and $\alpha = 45^\circ$); 57.9% (Ω_3 when $\beta = 0.5$, $\gamma = 2.5$ and $\alpha = 45^\circ$); 57.5% (Ω_2 when $\beta = 0.5$, $\gamma = 1$ and $\alpha = 45^\circ$) and 51.7% (Ω_7 when $\beta = 0.5$, $\gamma = 1$ and $\alpha = 45^\circ$). It can be seen that all the first five differences between the algebraic polynomial solutions and the present solutions occur at the skew angle $\alpha = 45^\circ$. Therefore, it can be concluded that the 3-D finite element solutions are agreement with the present solutions. However, the differences between the algebraic polynomial solutions and the present solutions are considerable for plates with large skew angles.

From Tables 3 to 8, one can see that for the cantilevered rectangular plates ($\alpha = 0^\circ$), all results obtained from the three methods are agreement each other, although the present solutions are, in general, closer to the 3-D finite element solutions. The maximum difference between the 3-D finite element solutions and the present solutions is 4.7% (Ω_4 when $\beta = 0.5$ and $\gamma = 1$) while the maximum difference between the algebraic polynomial solutions and the present solutions is 8.4% (Ω_4 when $\beta = 0.5$ and $\gamma = 2.5$). However, with the increase of the skew angle, the differences between the algebraic polynomial solutions and the present solutions monotonically and remarkably increase and greatly larger than the differences between the finite element solutions and the present solutions. It should be mentioned that McGee and Leissa [30] examined the convergence of the algebraic polynomial solutions for the cantilevered rhombic plate ($\beta = 1$) with the skew angle $\alpha = 15^\circ$. They reported that the algebraic polynomials led to serious round-off errors as the solution

Table 8
The first eight frequency parameters for skewed, cantilevered thick plates with aspect ratio $\beta = 2$ and span-thickness ratio $\gamma = 10$

Mode	Method	$\alpha = 0^\circ$	$\alpha = 15^\circ$	$\alpha = 30^\circ$	$\alpha = 45^\circ$
Ω_1	Present	3.3997	3.4640	3.6545	3.9568
	Ref. [30]	3.3397	3.3432	3.0183	2.9961
	3-D FE	3.4114	3.5002	3.7805	4.3144
Ω_2	Present	13.2935	13.5040	13.7016*	12.4847*
	Ref. [30]	12.4593	12.5382	12.7095	11.6690
	3-D FE	13.2833	13.5085	13.8810	12.9673
Ω_3	Present	14.4057*	14.2514*	14.2949	16.1251
	Ref. [30]	14.3907	14.4765	15.4606	16.0299
	3-D FE	14.4521	14.3258	14.4257	16.6212
Ω_4	Present	20.2979	20.9298	22.7865	25.8173
	Ref. [30]	19.5960	19.7466	20.6890	23.6116
	3-D FE	20.3647	21.1291	23.4390	27.4966
Ω_5	Present	41.9258	41.4907	41.5081	43.8744
	Ref. [30]	38.7711	37.5107	35.3326	35.6590
	3-D FE	41.9086	41.6010	42.1593	46.0781
Ω_6	Present	52.2346*	50.6208*	48.5529*	46.4501*
	Ref. [30]	52.2825	49.9046	51.9786	64.1992
	3-D FE	52.3346	50.6122	48.6333	47.2957
Ω_7	Present	53.3858	55.6505	59.3579*	60.6123*
	Ref. [30]	52.4692	50.3584	55.3036	68.8087
	3-D FE	53.4834	55.9763	59.9545	62.1115
Ω_8	Present	54.8204*	56.7512*	61.5335	68.9504
	Ref. [30]	54.8140	54.0790	57.9550	71.5920
	3-D FE	54.7376	56.9011	62.7143	72.3215

Note: Data with superscript (*) mean the symmetric modes in the thickness direction.

determinant sizes became larger than 288 which corresponds to $I \times J \times K = 6 \times 4 \times 4$. In their subsequent computations, 288 terms of algebraic polynomials was constantly applied to the computations of cantilevered skew plates with various skew angles including larger skew angles such as $\alpha = 30^\circ$ and $\alpha = 45^\circ$. The present study shows that with the increase of the skew angle, the maximum number of terms of the trial functions, which could provide the stable numerical computation, should monotonically decrease. Therefore, $I \times J \times K = 6 \times 4 \times 4$ terms of algebraic polynomials will give the ill-conditioned results for plates with larger skew angles such as $\alpha = 45^\circ$. This also explains the reason why the first five remarkable differences between the algebraic polynomial solutions and the present solutions always occur at the skew angle $\alpha = 45^\circ$.

The 3-D finite element solutions in Tables 3–8 are directly cited from reference [30] where the commercial software NASTRAN was used to obtain the finite element results. McGee and Leissa [30] investigated the convergence of the 3-D finite element solutions and pointed that the mesh refinement does not always reduce the error of the 3-D finite element results and utilization of large number of elements does not necessarily lead to closer results. The above study indicates that the present method could provide more accurate results than the finite element method.

Figs. 3–5 give the vibration modes of cantilevered skew plates with the aspect ratio $\beta = 1$ and skew angle $\alpha = 30^\circ$. The first six modes for three different span-thickness ratios $\gamma = 2$, 5, 20 are presented, respectively. It is seen from Figs. 3 to 5 that the antisymmetric modes in the thickness direction exhibit the flexural vibrations while the symmetric modes in the thickness direction exhibit the extending vibrations. With the increase of the plate thickness, the symmetric modes in the thickness direction go into the low-order eigenfrequencies.

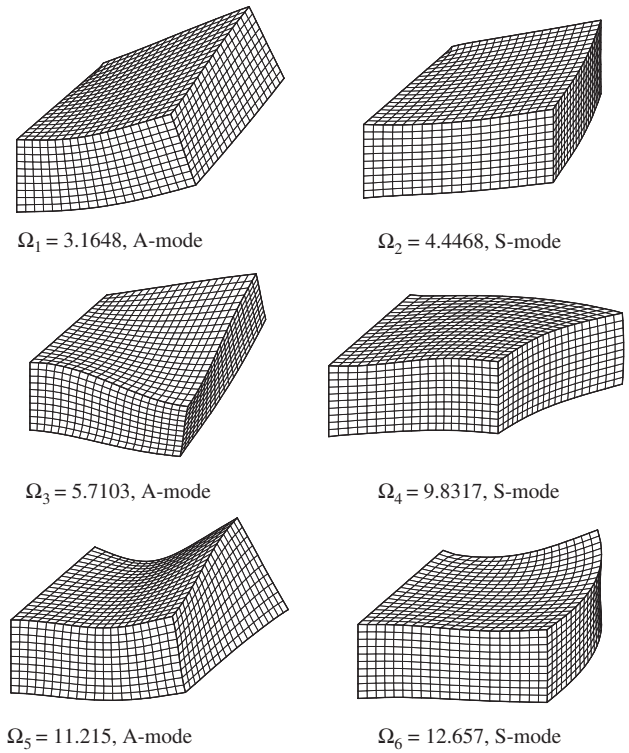

Fig. 3. The first six modes of cantilevered skew plate with, $\alpha = 30^\circ$. A-mode means antisymmetric mode and S-mode means symmetric mode.

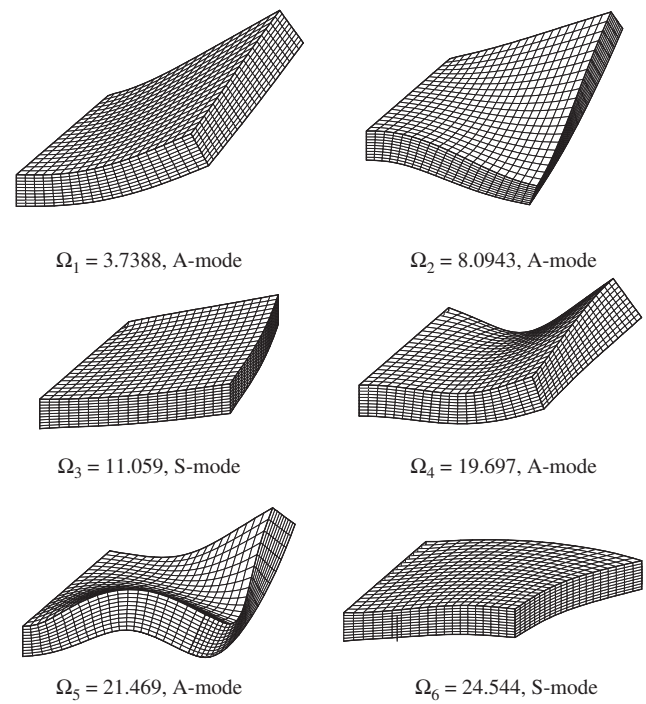

Fig. 4. The first six modes of cantilevered skew plate with $\beta = 1.0$, $\gamma = 5.0$, $\alpha = 30^\circ$. A-mode means antisymmetric mode and S-mode means symmetric mode.

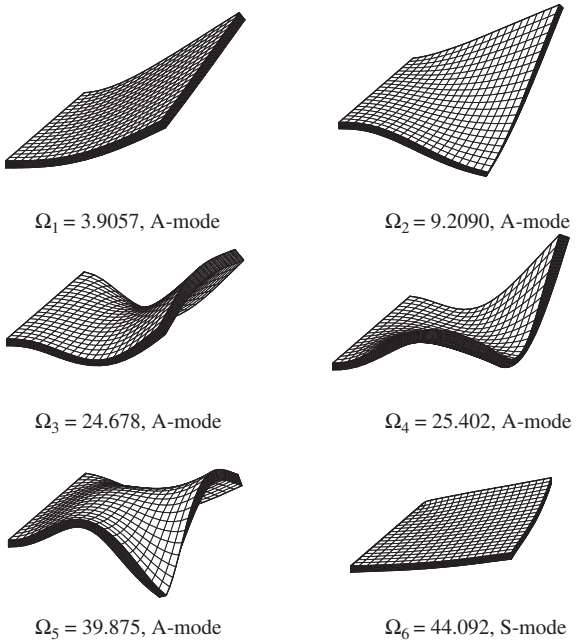

Fig. 5. The first six modes of cantilevered skew plate with $\beta = 1.0$, $\gamma = 20.0$, $\alpha = 30^\circ$. A-mode means antisymmetric mode and S-mode means symmetric mode.

5. Conclusions

The 3-D free vibration of cantilevered skew plates with arbitrary thickness has been solved using the Ritz method. The solution is based on the exact, linear and small strain elasticity theory. The triplicate Chebyshev polynomial series multiplied by a boundary characteristic function are used as the trial functions. High accuracy and rapid convergence demonstrate the advantage of using Chebyshev polynomials as the trial functions. Reliable frequency parameters have been obtained for cantilevered skew plates with various aspect ratios, span-thickness ratios and skew angles. The comparison study clearly shows that the present solutions are in agreement with the 3-D finite element solutions for all cases, however in some cases, are inconsistent with the algebraic polynomial solutions, especially for plates with large skew angles such as $\alpha = 45^\circ$. It can be concluded that in 3-D vibration analysis of skew thick plates, the numerical stability of using Chebyshev polynomials as the trial functions is better than that of using algebraic polynomials as the trial functions. The present results can serve as the benchmark data for the accuracy evaluation of other computational techniques.

References

[1] S.P. Timoshenko, S. Woinowsky-Krieger, *Theory of Plates and Shells*, McGraw-Hill, New York, 1959.
[2] R.D. Mindlin, Influence of rotatory inertia and shear on flexural motions of isotropic elastic plates, *ASME Journal of Applied Mechanics* 18 (1951) 31–38.
[3] J.N. Reddy, A simple higher-order theory for laminated composite plates, *ASME Journal of Applied Mechanics* 51 (1984) 745–752.
[4] M.V. Barton, Vibration of rectangular and skew cantilever plates, *ASME Journal of Applied Mechanics* 18 (1951) 129–134.
[5] R.K. Kaul, V. Cadambe, The natural frequencies of thin, skew plates, *Aeronautical Quarterly* 7 (1956) 337–352.
[6] S. Durvaaula, Natural frequencies and modes of skew membranes, *Journal of Acoustical Society of America* 44 (1968) 1636–1646.
[7] S. Durvasula, Natural frequencies and modes of clamped skew plates, *AIAA Journal* 7 (1969) 1164–1167.
[8] P.S. Nair, S. Durvasula, Vibration of skew plates, *Journal of Sound and Vibration* 26 (1973) 1–19.
[9] T. Mizusawa, T. Kajita, M. Naruoka, Vibration of skew plates by using B-spline functions, *Journal of Sound and Vibration* 62 (1979) 301–308.

[10] K.M. Liew, K.Y. Lam, Application of two-dimensional orthogonal plate function to flexural vibration of skew plates, *Journal of Sound and Vibration* 139 (1990) 241–252.
[11] D.J. Gorman, Accurate analytical-type solutions for the free-vibration of simply-supported parallelogram plates, *ASME Journal of Applied Mechanics* 58 (1991) 203–208.
[12] N.S. Bardell, The free vibration of skew plates using the hierarchical finite element method, *Computers and Structures* 45 (1992) 841–874.
[13] O.G. McGee, A.W. Leissa, C.S. Huang, Vibrations of cantilevered skewed plates with corner stress singularities, *International Journal for Numerical Methods in Engineering* 35 (1992) 409–424.
[14] C.S. Huang, O.G. McGee, A.W. Leissa, J.W. Kim, Accurate vibration analysis of simply supported rhombic plates by considering stress singularities, *ASME Journal of Vibration and Acoustics* 117 (1995) 245–251.
[15] K. Kanaka Raju, E. Hinton, Natural frequencies and modes of rhombic Mindlin plates, *Earthquake Engineering and Structural Dynamics* 8 (1980) 55–62.
[16] N. Ganesan, Nagaraja Rao, Vibration analysis of moderately thick skew plates by a variational approach, *Journal of Sound and Vibration* 101 (1985) 117–119.
[17] C.M. Wang, Natural frequencies formula for simply supported Mindlin plates, *ASME Journal of Vibration and Acoustics* 116 (1994) 536–540.
[18] W.H. Wittrick, Analytical three-dimensional elasticity solutions to some plate problems, and some observations on Mindlin's plate theory, *International Journal of Solids and Structures* 23 (1987) 441–464.
[19] C.W. Lim, Three-dimensional vibration analysis of a cantilevered parallelepiped: exact and approximate solutions, *Journal of Acoustical Society of America* 106 (1999) 3375–3381.
[20] S. Srinivas, C.V.J. Rao, A.K. Rao, An exact analysis for vibration of simply-supported homogeneous and laminated thick rectangular plates, *Journal of Sound and Vibration* 12 (1970) 187–199.
[21] J.R. Hutchinson, S.D. Zillimer, Vibration of a free rectangular parallelepiped, *ASME Journal of Applied Mechanics* 50 (1983) 123–130.
[22] A. Fromme, A.W. Leissa, Free vibration of the rectangular parallelepiped, *Journal of Acoustical Society of America* 48 (1970) 290–298.
[23] A.W. Leissa, Z.D. Zhang, On the three-dimensional vibrations of the cantilevered rectangular parallelepiped, *Journal of Acoustical Society of America* 73 (1983) 2013–2021.
[24] Y.K. Cheung, S. Chakrabarti, Free vibration of thick, layered rectangular plates by a finite layer method, *Journal of Sound and Vibration* 21 (1972) 277–284.
[25] M. Malik, C.W. Bert, Three-dimensional elasticity solutions for free vibrations of rectangular plates by the differential quadrature method, *International Journal of Solids and Structures* 35 (1998) 231–299.
[26] K.M. Liew, T.M. Teo, Three-dimensional vibration analysis of rectangular plates based on differential quadrature method, *Journal of Sound and Vibration* 220 (1999) 577–599.
[27] D. Zhou, Y.K. Cheung, F.T.K. Au, S.H. Lo, Three-dimensional vibration analysis of thick, rectangular plates using Chebyshev polynomial and Ritz method, *International Journal of Solids and Structures* 39 (2002) 6339–6353.
[28] K.M. Liew, K.C. Hung, M.K. Lim, A continuum three-dimensional vibration analysis of thick rectangular plates, *International Journal of Solids and Structures* 30 (1993) 3357–3379.
[29] Y.K. Cheung, D. Zhou, Three-dimensional vibration analysis of cantilevered and completely free isosceles triangular plates, *International Journal of Solids and Structures* 39 (2002) 673–687.
[30] O.G. McGee, A.W. Leissa, 3-dimensional free-vibrations of thick skewed cantilevered plates, *Journal of Sound and Vibration* 144 (1991) 305–322.
[31] K.M. Liew, K.C. Hung, M.K. Lim, Three-dimensional elasticity solutions to vibration of cantilevered skewed trapezoids, *AIAA Journal* 32 (1994) 2080–2089.
[32] K.M. Liew, K.C. Hung, M.K. Lim, Vibration characteristics of simply supported thick skew plates in three-dimensional setting, *ASME Journal of Applied Mechanics* 62 (1995) 880–886.
[33] L. Fox, I.B. Parker, *Chebyshev Polynomials in Numerical Analysis*, Oxford University Press, London, 1968.